FINITE ELEMNT ANALYSIS FOR EVALUATION OF SLOPE STABILITY INDUCED BY CUTTING

Toshinori SAKAI
Department of Environmental Science and Technology, Mie University, Tsu, Japan
Tadatsugu TANAKA
Graduate School of Agriculture and Life Science, University of Tokyo, Tokyo Japan

***ABSTRACT*:** This paper concerned an evaluation of stability condition of slope. A slope stability induced by cutting was evaluated by a finite element analysis. The finite element analysis employed a constitutive model in which non-associated strain hardening-softening elasto-plastic material was assumed. In-site investigation was done by an inclinometer for the boreholes. For defining the soil stratum, a new data processing system was applied in this paper to generate a soil ground model, using many boring data. Soil samples were taken and subjected to geotechnical laboratory tests. A triaxial compression test ($\overline{CU}$) was performed to determine the shear strength. The numerical analysis did not consider the pore pressure, because no ground water was appeared in that area. The deformation obtained by the numerical analysis was close to the results of inclinometer of borehole observed by in-site investigation. The finite element analysis was able to predict the estimation of the slope stability induced by cutting.

***KEYWORDS*:** Slope stability, Finite element analysis, In-site investigation

1. INTRUDUCTION

In more than 70% of Shikoku Island, there are many steep slope in a mountainous district. There are many landslides in the central part of Shikoku Island where is composed of crystalline schist of Sambagawa metamorphic belt. Slope failure is often caused by the cutting or filling in this area. The evaluation of slope stability is mainly used by an analysis that is based on rigid-plasticity theory. This analysis involves arbitrary assumptions regarding the shape of failure surface. The determination of the failure surface is dependent on the knowledge of experts who have a lot of experiences. However, it is difficult to determine the failure surface for the people having no expert knowledge.

Cutting or filling is performed in the steep mountain area to create plane sites. It is important to evaluate the influence of cutting or filling on the geotechnical behavior in the ground. In recent years, a finite element method is applied to the slope stability analysis. Ukai(1989) introduced the method of finite element analysis for landslide. Hoshikawa *et al* (1999) reported the excavation analysis of vertical cutting. The ground deformation by cutting on the slope was predicted by using the finite element

method (Zienkiewicz *et al*, 1975). Tanaka and Kawamoto (1989) proposed the finite element analysis in which non-associated strain hardening-softening elasto-plastic material was assumed. The analytical method is able to apply to the design of civil engineering constructions (Sakai *et al*, 1998, 1999).

The present article attempts to explain the stability of slope induced by cutting, comparing the results of finite element analysis with the same from experimental in-site investigation.

2. LANDSILDE CHARACTERIZATION

The location of Shikoku Island and place of investigation are shown in Fig.1. This area is composed of crystalline schist of Sanbagawa metamorphic belt. An inclination of the slope was around 25 degrees and an orange was cultivated on that slope. When the cutting slope was done, a lot of cracks occurred on a surface of road which was a top of the cutting slope as shown in Fig.2(a). A general view of a landslide area before and after cutting is shown in Fig.3. There are 19 boring logs with SPT (Standard Penetration Test) in this area. The borehole core and N value of bore hole No.7 are shown in Fig.4. The bedrock appears exceeding 8.5m below the ground level at bore hole No.7. From in-site investigation, the sliding layer was observed to exist above the bedrock and the thickness of sliding layer was about 50cm (Fig.2(b)). The deformation observed by the inclinometer of borehole No.7 is shown in Fig.5. It appeared that the sliding surface positioned around 8.5m below the ground level with SE direction. Section B-B (Fig.3) corresponds to the result of the inclinometer of borehole No.7. Section A-A (Fig.3) is a maximum inclined angle on the slope. No ground water was appeared and its level was under the sliding surface.

Fig.1 Location of Shikoku Island and place of investigation

(a) Craks on the road

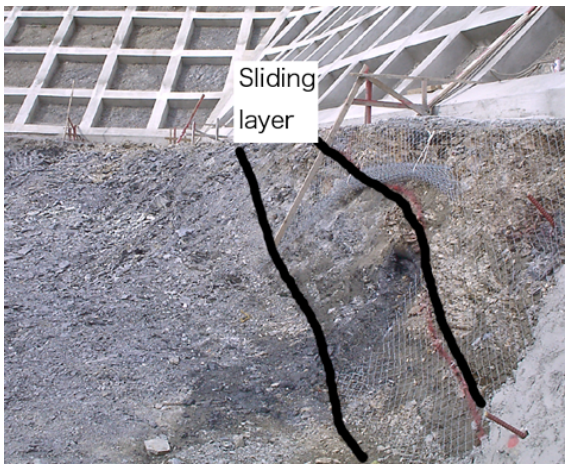

(b) View of the sliding layer

Fig.2 Condition of investigation site

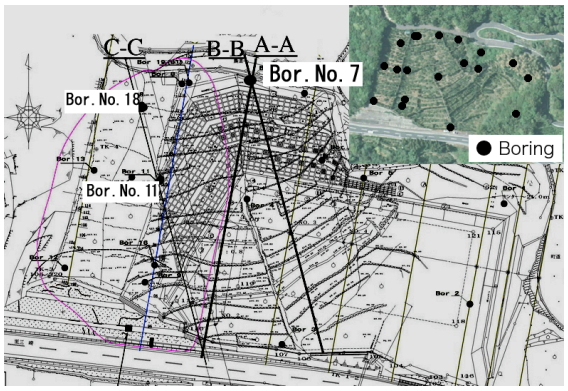

Fig.3 A general view of the site

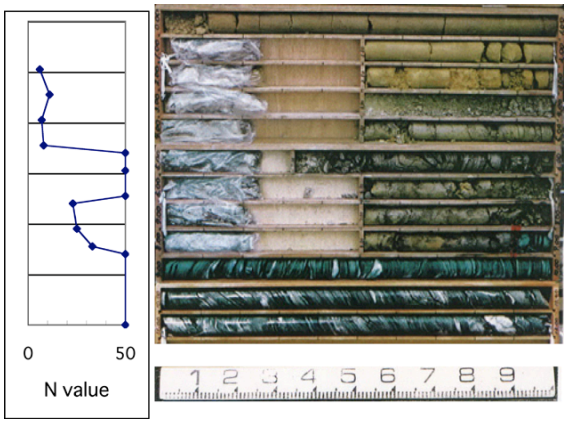

Fig.4 Borehole core and N Vale of Bor. No.7

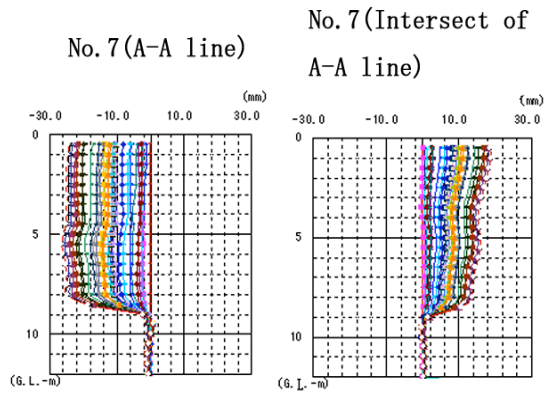

Fig.5 Displacement of inclinometer of Bor. No.7

Although, it is difficult to define soil stratum, this paper applies a new data processing system to generate a soil ground model using the many boring data (Tanaka *et al*, Sakajo and Tanaka, 2004). A 3D prediction of the soil stratum in that area is shown in Fig.6. The cross sections of A-A and B-B are shown in Fig.7.

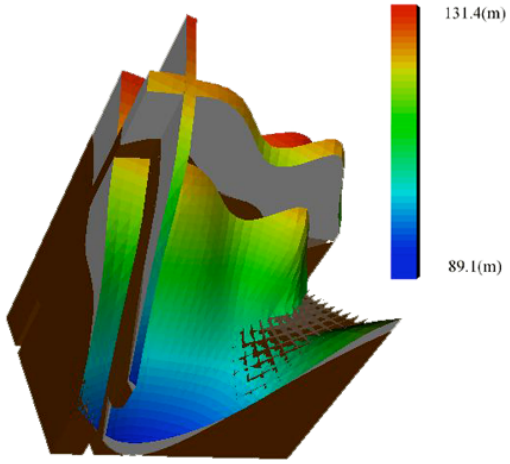

Fig.6 3D prediction of the soil stratum

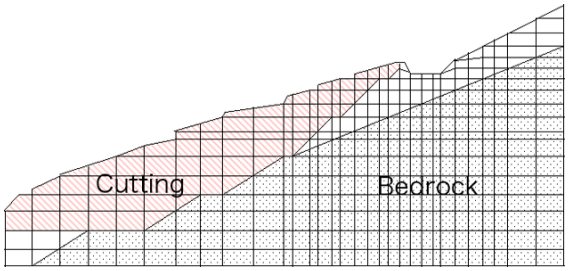

(a) Cross section of A-A

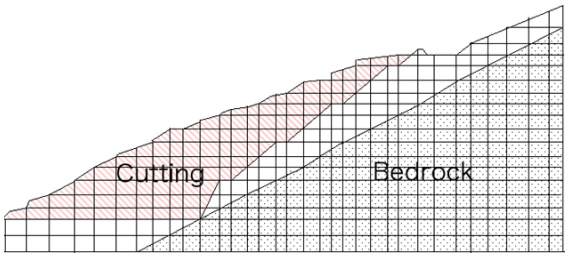

(b) Cross section of B-B

Fig.7 Cross section and finite element mesh

3. LABORATORY TEST

Undisturbed sample lay around the sliding surface was taken from the cutting slope surface. The physical properties of the sample are summarized in

Table 1. The grain size distribution curve is shown in Fig.8. In order to investigate the relationship between peak strength of the material, triaxial compression test ($\overline{CU}$) was conducted. The internal friction angle and cohesion were 25 degrees and 12.5kN/m^2, respectively. Yatabe (2004) reported that a residual friction angle of clay of crystalline schist of Sambagawa metamorphic belt was about 15 degrees.

Table 1 Physical properties of soil of sliding layer

ρ_s(g/cm^3)	ρ_t(g/cm^3)	W(%)	WL(%)	WP(%)	IP
2.756	2.46	14.19	41.21	22.22	18.99

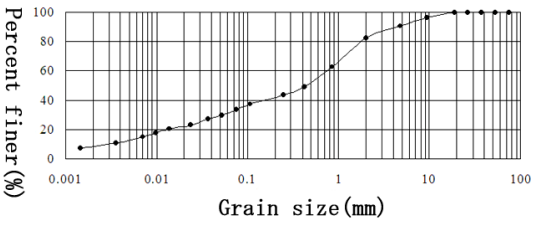

Fig.8 Grain size distribution of soil of sliding layer

4. NUMERICAL METHOD

For the analysis, an elasto-plastic model with non-associated flow rule and strain hardening -softening yield properties was used for the constitutive model. The yield function of Mohr-Coulomb model and plastic potential function of Drucker-Prager model were employed. The element was a pseudo-equilibrium model formed by one-point integration of a 4-noded isoparametric element. The modified Newton-Raphson iteration method was applied in the solution of non-linear analysis.

The yield function (f) and the plastic potential function (Ψ) are given by the following expression:

$$f = \frac{\sqrt{J_2}}{g(\theta)} + 3\alpha(\kappa)\sigma_m - \gamma(\kappa) = 0 \qquad (1)$$

$$\Psi = \sqrt{J_2} + 3\alpha'(\kappa)\sigma_m - \gamma'(\kappa) = 0 \qquad (2)$$

In a case of Mohr-Coulomb material, $g(\theta)$ takes the form:

$$g(\theta) = \frac{3 - sin\phi_{mob}}{2\sqrt{3}\cos\theta - 2sin\theta sin\phi_{mob}} \qquad (3)$$

where ϕ_{mob} is the mobilized friction angle and θ is the Lode angle.

The frictional hardening-softening functions are expressed as:

$$\alpha(\kappa) = \left\{\frac{2\sqrt{\kappa\varepsilon_f}}{\kappa + \varepsilon_f}\right\}^m \alpha_p \quad \text{(hardening-regime)} \qquad (4)$$

$$\alpha(\kappa) = \alpha_r + (\alpha_p - \alpha_r)\exp\left\{-\left(\frac{\kappa - \varepsilon_f}{\varepsilon_r}\right)^2\right\}$$

(softening-regime) (5)

where m, ε_f, ε_r are material parameter

$$\alpha_p = \frac{2sin\phi_p}{\sqrt{3}(3 - sin\phi_p)} \qquad (6)$$

$$\alpha_r = \frac{2sin\phi_r}{\sqrt{3}(3 - sin\phi_r)} \qquad (7)$$

where peak and residual friction angles are 25 and 15 degrees.

The mobilized friction angle (ϕ_{mob}) is expressed as:

$$\phi_{mob} = sin^{-1}\left(\frac{3\sqrt{3}\alpha(\kappa)}{2 + \sqrt{3}\alpha(\kappa)}\right) \qquad (11)$$

$\alpha'(\kappa)$ in plastic potential function is expressed as:

$$\alpha'(\kappa) = \frac{2sin\psi}{\sqrt{3}(3 - sin\psi)} \tag{12}$$

The dilatancy angle (ψ) can be estimated from modified Row's stress-dilatancy relation:

$$sin\psi = \frac{sin\phi_{mob} - sin\phi'_r}{1 - sin\phi_{mob} sin\phi'_r} \tag{13}$$

ϕ'_r is expressed as:

$$\phi'_r = \phi_r \left[1 - \beta \exp\left\{-\left(\frac{\kappa}{\varepsilon_d}\right)^2\right\}\right] \tag{14}$$

where β and ε_d are material parameters.

The cohesion $\gamma(\kappa)$ can be estimated from the following expression:

$$\gamma(\kappa) = \gamma_p \exp\left\{-\left(\frac{\kappa}{\varepsilon_c}\right)^2\right\} \tag{15}$$

$$\gamma_p = \frac{6C\cos\phi_p}{\sqrt{3}(3 - sin\phi_p)} \tag{16}$$

where C is cohesion and ε_c is material parameter.

The material parameters used in the analysis are listed in Table 2. The back-prediction of a triaxial compression test ($\overline{CU}$) by the finite element method using one element (5cm × 10cm) was carried out employing the material properties (Fig.9). The parameters of bedrock are the data from Tanaka and Kawamoto (1989).

Table 2 Material parameters

	non Bedrock	Bedrock
Density (ρ_t : g/cm^3)	2.5	2.5
Void ratio (e)	0.5	0.5
Cofficient of shear modulus (G_0)	50	2000
Residual friction angle (ϕ_r : deg.)	15.0	0.0
Peak friction angle (ϕ_p : deg.)	25.0	0.0
Poisson's ratio (ν)	0.3	0.3
Cohesion(kN/m^2)	12.5	0.0
ε_f	0.6	
ε_r	0.6	
m	0.3	
ε_c	0.6	
ε_d	0.3	
β	0.2	

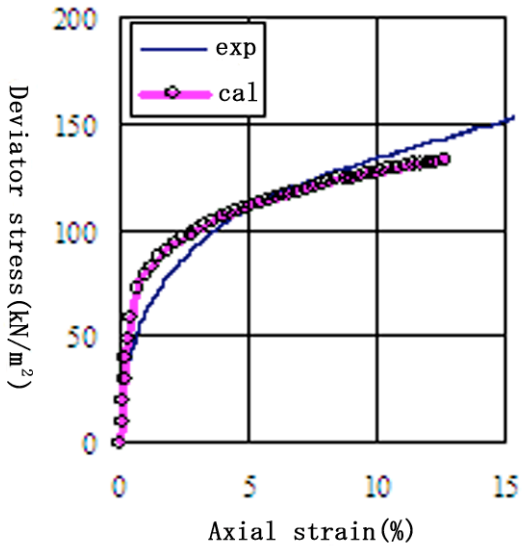

Fig.9 Simulated triaxial test ($\sigma_3 = 49kN/m^2$)

5. NUMERICAL RESULT

The deformations of slopes after cutting on the section A-A and section B-B are shown in Fig.10. In these figures, the nodal points of + and ● mean the position of initial and after cutting state. These figures show numerical results, which are close to position of deformations observed by the inclinometer for borehole No.7. The shape of sliding surface coincided with the dotted line shown in Fig.10. It was observed a lot of cracks appeared on the surface of road which was at the top of cutting slope. The sliding surface obtained by the finite element analysis coincided with the in-site investigations. The safety factor was carried out along section A-A and B-B. It was 0.94 along section A-A and was 0.84 along section B-B. From the results, the direction of movement for the slope by cutting was prevalently along section B-B.

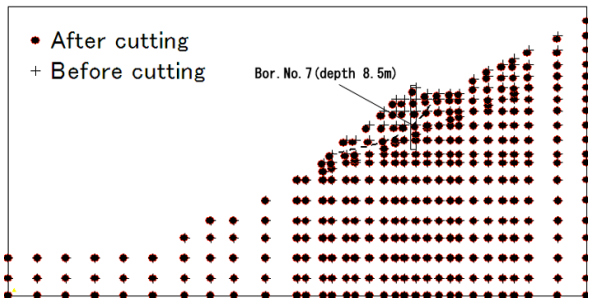

(a) Section A-A

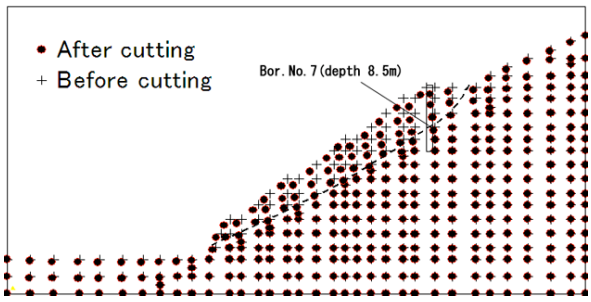

(b) Section B-B

Fig.10 Deformation of slope after cutting

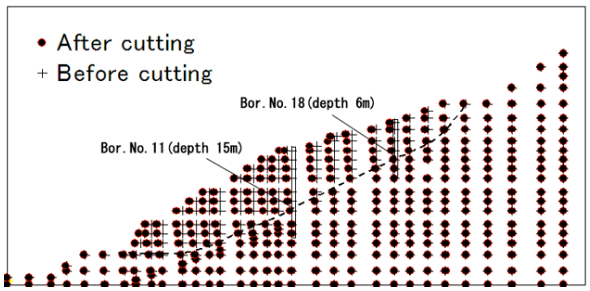

Fig.11 Deformation of slope after cutting
(Section C-C)

The deformation of slope induced by cutting along section C-C obtained by the finite element analysis is shown in Fig.11. There were two boreholes (No.11 and No.18) along the section. It appeared that the sliding surfaces positioned around 15m and 6m below the ground level for borehole No.11 and No.18, respectively. The shape of sliding surface was estimated as the dotted line shown in Fig.11. The deformation of slope obtained by in-site investigations agreed with the sliding surface obtained from numerical calculation. From the results, it is possible to predict the sliding surface by the finite element analysis.

6. CONCLUSION

This paper describes the evaluation of stability condition of slope induced by cutting. It is shown that the deformation calculated by the numerical analysis is close to in-site experimental investigation in the borehole. Therefore, it can be concluded that the finite element analysis is possible to predict the estimation of the slope stability induced by cutting.

Acknowledgment

This work has been partly supported by a Research Grant No.17380140 with funds from Grant-in-Aid for Science Research given by the Japanese Government. The author is very grateful to Prof. Takagi, Dr. Sakajo and Mr. Nishioka for their co-operation.

REFERENCES

T. Hoshikawa, T. Nakai and T. Nishi, Couple excavation analyses of vertical cut and slope in clay, *Proc. Int. Symp. Slope Stability Engineering*, Matsuyama, pp. 225-231, 1999

T. Tanaka and O. Kawamoto, Plastic collapse analysis of slopes of strain-softening materials. *Proc. 3rd Int. Conf. Numerical Models in Geomechanics*, pp. 667-674, 1989

Ukai, K., 1989, A method of calculation of total safety factor of slope by elasto-plastic FEM, *Soils and Foundations*, 29(2): 190-195.

Sakai, T. and Tanaka, T., 1998, Scale effect of a shallow circular anchor in dense sand, *Soils and Foundations*, 38(2): 93-99.

Sakai, T., Erizal and Miyauchi, S., 1999, Study of a progressive failure and a scale effect in retaining wall problem on passive mode, *Tans of JSIDRE*, 202: 7-13.

Sakajo, S. and Tanaka, M., 2004, Report of a new composite system for soil ground modeling. (in Japanese).

Tanaka, M., Watanabe, Y., Miyata, M. and Sakajo, S., 3D-Visualization of Ground of New Runway at Haneda Airport, *Soils and Foundations*, (now printing)

Yatabe, R. 2004, Report of the residual friction angle of crystalline schist of Sambagawa metamorphic belt, (in Japanese).

Zienkiewicz, O. C., Humpheson, C. and Lewis, R. W., 1975, Associated and non-associated visco-plasticity and plasticity in soil mechanics, *Geotechnique.* 25(4): 671-689.